Petroleum Science 21 (2024) 1018–1031

Contents lists available at ScienceDirect

Petroleum Science

journal homepage: www.keaipublishing.com/en/journals/petroleum-science

Original Paper

Hydrocarbon gas huff-n-puff optimization of multiple horizontal wells with complex fracture networks in the M unconventional reservoir

Hao-Chuan Zhang [a], Yong Tang [a], You-Wei He [a, *], Yong Qin [b], Jian-Hong Luo [c], Yu Sun [a], Ning Wang [a], De-Qiang Wang [d]

[a] State Key Laboratory of Oil and Gas Reservoir Geology and Exploitation, Southwest Petroleum University, Chengdu, 610500, Sichuan, China
[b] CNPC Research Institute of Petroleum Exploration & Development, Beijing, 100083, China
[c] Southwest Oil & Gas Field Company, PetroChina, Chengdu, 610051, Sichuan, China
[d] State Key Laboratory of Offshore Oil Exploitation, CNOOC Research Institute Co. Ltd, Beijing, 100027, China

ARTICLE INFO

Article history:
Received 21 June 2023
Received in revised form
17 October 2023
Accepted 30 October 2023
Available online 5 November 2023

Edited by Yan-Hua Sun

Keywords:
Unconventional oil reservoir
Complex fracture network
Hydrocarbon gas huff-n-puff
Parameter optimization
Numerical simulation

ABSTRACT

The oil production of the multi-fractured horizontal wells (MFHWs) declines quickly in unconventional oil reservoirs due to the fast depletion of natural energy. Gas injection has been acknowledged as an effective method to improve oil recovery factor from unconventional oil reservoirs. Hydrocarbon gas huff-n-puff becomes preferable when the CO_2 source is limited. However, the impact of complex fracture networks and well interference on the EOR performance of multiple MFHWs is still unclear. The optimal gas huff-n-puff parameters are significant for enhancing oil recovery. This work aims to optimize the hydrocarbon gas injection and production parameters for multiple MFHWs with complex fracture networks in unconventional oil reservoirs. Firstly, the numerical model based on unstructured grids is developed to characterize the complex fracture networks and capture the dynamic fracture features. Secondly, the PVT phase behavior simulation was carried out to provide the fluid model for numerical simulation. Thirdly, the optimal parameters for hydrocarbon gas huff-n-puff were obtained. Finally, the dominant factors of hydrocarbon gas huff-n-puff under complex fracture networks are obtained by fuzzy mathematical method. Results reveal that the current pressure of hydrocarbon gas injection can achieve miscible displacement. The optimal injection and production parameters are obtained by single-factor analysis to analyze the effect of individual parameter. Gas injection time is the dominant factor of hydrocarbon gas huff-n-puff in unconventional oil reservoirs with complex fracture networks. This work can offer engineers guidance for hydrocarbon gas huff-n-puff of multiple MFHWs considering the complex fracture networks.

1. Introduction

Unconventional oil reservoirs are widely distributed with abundant reserves and high potential. Accordingly, efficient exploitation of unconventional oil resources can ensure energy supply and safety (Bealessio et al., 2021; Hu et al., 2018). However, the formation pressure in unconventional oil reservoirs drops quickly after production due to narrow throat radius, and partial closure of micro-fractures can reduce the fluid flow ability (Wang and Zhang, 2018; Ding et al., 2019; Jing et al., 2021).

Horizontal wells are designed to increase the controlled reserves by increasing contacting regions between the formation and horizontal wellbore (Cheng et al., 2017; He et al., 2020; Fu et al., 2023). Multistage hydraulic fracturing can achieve adequate fluid flow from matrix to horizontal wellbore by generating complicated networks composed of natural and hydraulic fractures (Zhao et al., 2014; Chen et al., 2020; Zhang et al., 2022; He et al., 2023a; Qin et al., 2023). Thus, multi-fractured horizontal well (MFHW) technology is widely applied in unconventional reservoirs to obtain commercial productivity (Ming et al., 2020; Zhang and Yang, 2021; He et al., 2023b).

Water injection and gas injection have been widely used in oil reservoirs to avoid rapid decline in oil production (Feng et al., 2019; Wang et al., 2021; He et al., 2022; Tang et al., 2022). However, water

* Corresponding author.
E-mail address: youweihe_cupb@163.com (Y.-W. He).

https://doi.org/10.1016/j.petsci.2023.10.026

sensitivity during water injection may lead to formation damage (Zhao et al., 2016; Sun et al., 2022). In the process of unconventional oil reservoir exploitation, gas injection can avoid damaging the formation and effectively enhance oil recovery (EOR) (Sumeer et al., 2018; Tang et al., 2021a; Ding et al., 2022; Lei et al., 2023). Though CO_2 is generally used for gas injection, large-scale CO_2 injection cannot be implemented due to the shortage of CO_2 gas sources in some regions. CO_2 source is hard to obtain and the cost is expensive in the M oilfield. Hydrocarbon gas is easily available and can be separated from the produced gas (Fu et al., 2021). Moreover, hydrocarbon gas is difficult to react physically and chemically with rocks and can be recycled for economic benefits (Cockin et al., 2000; Yan et al., 2023). It is difficult to establish the patterns of gas flooding since the significant difference in injection and production pressure in unconventional oil reservoirs. Therefore, hydrocarbon gas huff-n-puff is an essential means for unconventional oil reservoirs (Tang et al., 2021b). Hydrocarbon gas huff-n-puff has many advantages, such as fast payback, low investment and less gas channeling (Zheng et al., 2021; Sie and Nguyen, 2022). At present, gas huff-n-puff of horizontal wells are mainly used in thick oil reservoirs and complex fault block reservoirs (Hao et al., 2020; Ozowe et al., 2020). Thus, it is rare to study the hydrocarbon gas huff-n-puff optimization of multiple horizontal wells considering complex fracture networks.

The M oil reservoir is located in the northwest edge of the Junggar Basin, which has enormous oil production potential (Li et al., 2023). The M reservoir includes strong heterogeneity, poor physical properties, and significant horizontal stress difference (Wang et al., 2022; Xiong et al., 2022). Large-scale CO_2 huff-n-puff is less feasible in the M reservoir as a result of insufficient CO_2 sources. Hydrocarbon gas has similar characteristics to crude oil and is easy to achieve miscible displacement after gas injection. Therefore, hydrocarbon gas huff-n-puff are highly feasible for the M oil reservoir.

The dominant factors of gas huff-n-puff and the EOR mechanism are beneficial to efficient development of unconventional reservoirs. Haines and Monger (1990) studied hydrocarbon gas huff-n-puff to improve oil flooding efficiency, discovering that the increased oil from hydrocarbon gas huff-n-puff is affected by gas injection volume. The mechanism of increased oil includes increasing formation pressure as well as gas relative permeability hysteresis. Lino (1994) evaluated the natural gas huff-n-puff in light oil reservoirs in the Miranga field in Brazil, which illustrated that natural gas significantly improves oil production performance and is less costly than CO_2 huff-n-puff. Mohammed-Singh et al. (2006) first summarized the reservoir conditions suitable for CO_2 huff-n-puff by analyzing CO_2 huff-n-puff projects over the past 20 years and correlating different parameters with each other. Torabi and Asghari (2010) researched the performance of CO_2 for EOR and CO_2 storage in fractured porous media through physical simulation experiments. The studies show that the natural water saturation is favorable for CO_2 huff-n-puff under unmixed-phase conditions. In contrast, the impact on the process performance under mixed-phase conditions is almost negligible. Pu et al. (2016) investigated the effects of CO_2 on tight oil development through physical experiments. The results of huff-n-puff show that oil expansion coefficient and CO_2 solubility become higher by increasing pressure, and natural gas is primarily sensitive to differences in production pressure. Zhao et al. (2018) obtained that nitrogen foam huff-n-puff increases oil production by maintaining pressure, and the foaming agent can avoid the nitrogen gas channeling and expand the swept volume of gas, which effectively suppresses the influence of side water. Zhou et al. (2020) considered a random fractal geometry system and built random fractal fracture network model using dual-porosity. These studies showed that the oil recovery became higher by longer injection time and higher pressure, and an optimal injection timing existed for every gas huff-n-puff cycle.

The impact of complex fracture networks and well interference on hydrocarbon gas huff-n-puff of multiple MFHWs is unclear. Thus, this work focuses on hydrocarbon gas huff-n-puff optimization of multiple horizontal wells under complex fracture networks. A fine numerical model based on unstructured grids is developed to characterize the complex fracture networks and capture the dynamic fracture feature. The simulation of fluid phase behavior is carried out, and the numerical model of hydrocarbon gas huff-n-puff considering the complex fracture networks is established. Furthermore, parameter optimization of hydrocarbon gas huff-n-puff considering complex fracture networks is implemented using compositional numerical simulation. Ultimately, this work obtains the dominant factors of hydrocarbon gas huff-n-puff under complex fracture networks by using the fuzzy mathematical method. Fig. 1 shows the flowchart of this work.

2. Numerical model

2.1. Fluid phase behavior simulation

The PVTi module of Eclipse is used to calculate the critical parameters, providing a fluid model for the numerical simulation of hydrocarbon gas injection. The composition of the original formation fluid is divided and reorganized into seven pseudo-components, which can improve the calculation speed of numerical simulation and accurately characterize the properties of the formation fluid. The pseudo-components of the oil sample are shown in Table 1. The contrast of single flash experimental data with simulated data is shown in Table 2. The parameters are all within 5% of the error range. The calculation equation of the relative error is shown in Eq. (1). Table 3 shows the critical parameters from Eclipse after fitting the formation fluid model and its accuracy is essential for calculating the fluid phase behavior and physical properties in numerical simulation models.

$$R_e = \frac{|V_s - V_e|}{V_e} \times 100\%, \tag{1}$$

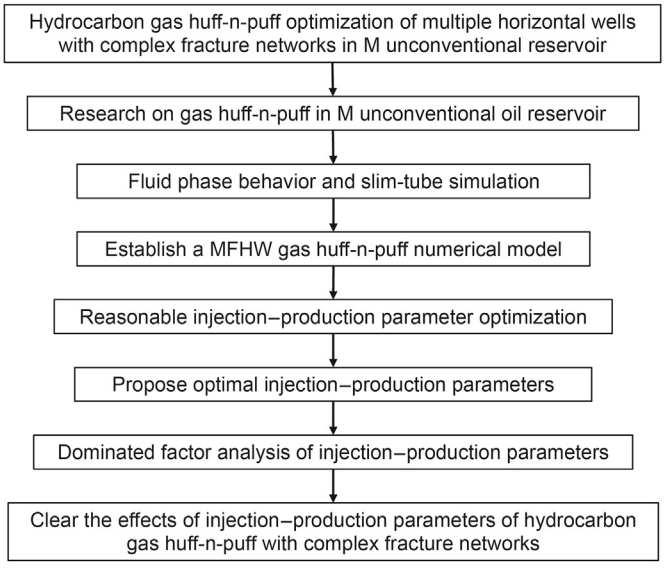

Fig. 1. Flowchart of this work.

Table 1
Pseudo-components of oil sample.

Pseudo-component	CO_2	N_2	CH_4	C_2–C_5	C_6–C_{10}	C_{11}–C_{37}	C_{38+}
Molar composition	0.0159	0.0004	0.1302	0.1139	0.2413	0.2759	0.2224

Table 2
Comparison of single flash experimental data with simulated data.

Property	Solution gas/oil ratio, m^3/m^3	Crude oil density, g/cm^3	Stock tank oil density, g/cm^3	Crude oil viscosity, mPa s	Saturation pressure, MPa
Experimental value	18.11	0.8	0.84	2	3.92
Simulated value	18.83	0.83	0.86	2.02	4.04
Relative error, %	3.98	3.75	2.38	1	3.06

Table 3
Critical parameters of the reservoir fluid components.

Pseudo-component	P_c, bar	T_c, °C	Z_c	Ω_A	Ω_B	Acentric factor	Molar weight
CO_2	73.866	31.55	0.274	0.457	0.078	0.225	44.01
N_2	33.944	−146.95	0.291	0.457	0.078	0.040	28.013
C_1	46.042	−82.55	0.285	0.457	0.078	0.013	16.043
C_{2+}	42.212	99.46	0.289	0.457	0.078	0.157	46.61
C_{6+}	27.172	311.81	0.256	0.457	0.078	0.337	113.77
C_{11+}	18.143	445.08	0.237	0.457	0.078	0.549	208.21
C_{38+}	5.698	692.73	0.141	0.457	0.078	1.442	675.84

where V_s is the simulated value; V_e is the experimental value; R_e is the relative error.

2.2. Simulation of slim tube

The slim-tube experimental results are used to develop the simulation model of the slim tube. The length of the tube is 20 m. The one-dimensional slim tube model with grid blocks of 50 × 1 × 1 is shown in Fig. 2. The model dimension is 20 m × 0.0034 m × 0.0034 m. This model includes one production well and one injection well. The temperature of the slim tube remains constant during the simulation (97.8 °C). Table 4 displays the oil recovery factor by injecting hydrocarbon gas under different pressures. The minimum miscible pressure (MMP) for the slim tube simulation can be found in Fig. 3.

The pressure is about 34.3 MPa when the oil recovery factor reaches 90%, which is the MMP of the slim-tube simulation. The results of the slim-tube simulation and the physical experiments are in good agreement (MMP is 33.5 MPa), which indicates that the fluid model can be used for the numerical model of hydrocarbon gas huff-n-puff. The reservoir pressure is 35 MPa. The pressure near the wellbore is increased after the hydrocarbon gas is injected into the formation and it becomes much higher than the MMP. Miscible displacement can be achieved at current pressure.

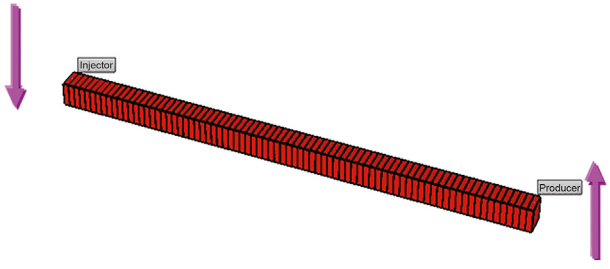

Fig. 2. One-dimensional slim tube model.

Table 4
Oil recovery factor by injecting hydrocarbon gas under different pressures.

Injection pressures, MPa	Oil recovery factor, %
26	69.1
29	78.6
32	85.5
35	92.5
38	95.9
41	97.9

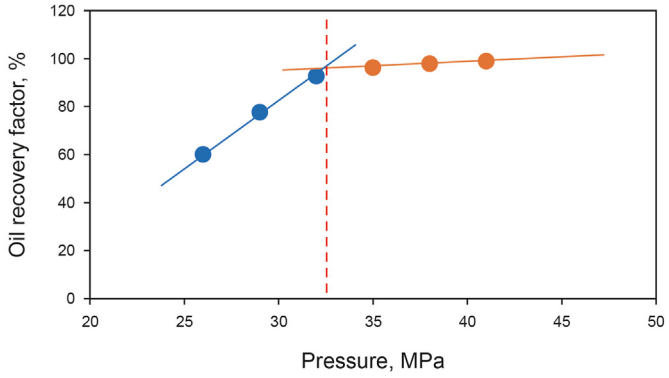

Fig. 3. The MMP for the slim-tube simulation.

2.3. Gas huff-n-puff numerical models considering complex fracture networks

Since rectangular grids cannot accurately describe the features of fractures, this work uses unstructured grids to characterize fractures with higher accuracy. Rectangular grids are chosen to characterize the matrix to reduce the number of grids. In order to accurately simulate the seepage between fractures and matrix, an MFHW hydrocarbon gas huff-n-puff model is established with considering complex fracture networks. The basic parameters of reservoir and wells can be seen in Table 5.

Table 5
Basic parameters of reservoir, wells and fluid.

Parameter	Value	Parameter	Value
Model size, m × m × m	2260 × 2260 × 48	Average permeability of matrix, mD	0.8
Model area, km^2	5.11	Number of fractures	195
Number of grids	76614 (113 × 113 × 6)	Porosity	0.06
Grid size, m × m × m	20 × 20 × 8	Initial reservoir pressure, MPa	55
Horizontal well length, m	1250	Reservoir temperature, °C	97.8
Reservoir depth, m	3500	Density of crude oil, t/m^3	0.8

(1) Numerical model gridding

The fractures are defined based on the results of micro-seismic monitoring, and unstructured grids are used to refine the grid near fractures. The rectangular grid is used in areas far from the horizontal wells to improve the speed of model calculations. The impression of reservoir boundaries during the hydrocarbon gas huff-n-puff should be avoided. The model dimension is 2260 m × 2260 m × 48 m, corresponding to length, width, and height. Among them, each matrix grid is set to 113 × 113 × 6, and the grid size is set to 20 m × 20 m × 8 m. The longitudinal stratification coefficient is set to 3. The micro-fracture size is set to 3 m. In the following images, Fig. 4 shows the planar grid, Fig. 5 shows the 3D grid of the well group model, and Fig. 6 shows the unstructured grid model of the fracture.

(2) Property model

By interpolating the interpretation data of single well logging, a property model is obtained. The logging interpretation shows that the permeability of the matrix reservoir is 1.18 mD, the permeability of the fractures is 104.6 mD, and the reservoir porosity is 6%. Fig. 7 displays the distribution of formation permeability, formation porosity, and oil saturation.

(3) Matrix and fracture zoning

During oil production, the stress-sensitive effects of fracture can impede the transfer of pressure drop funnels, thereby reducing the control range of the horizontal well. In order to get more accurate simulation results, the model considers the stress sensitivity of fractures and simulates the pressure drop pattern. The partitioning of fracture and matrix is shown in Fig. 8.

By setting different relative permeability and compressibility, the transfer between matrix and fracture can be better characterized. The proppant is set through a pumping procedure to improve fracture conductivity.

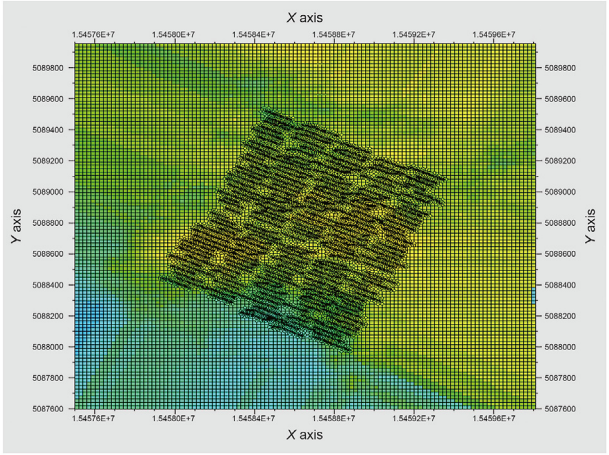

Fig. 4. The planar grid.

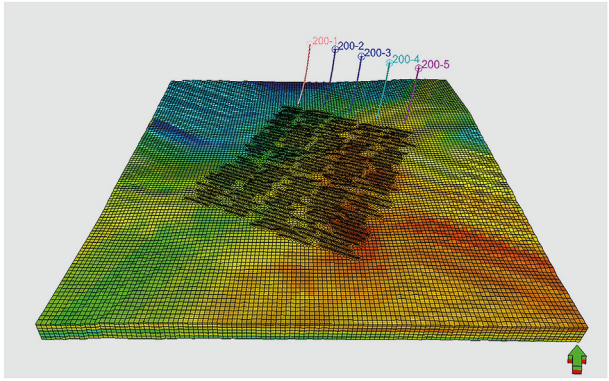

Fig. 5. The 3D grid of the well group model.

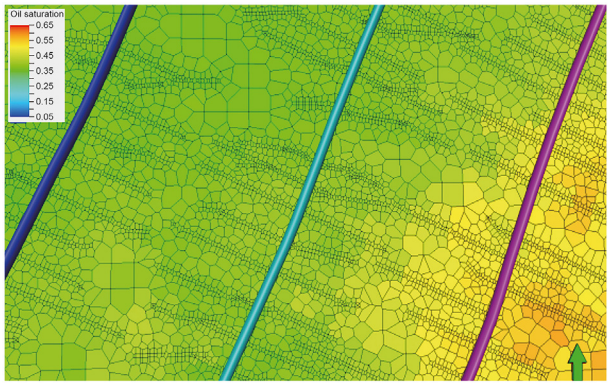

Fig. 6. The unstructured grid model of the complex fracture network.

(4) Fluid data

Formation fluid data is mimported into the numerical model. The initial conditions are set through equilibrium initialization, and the fluid component model for simulating gas huff-n-puff is established.

The geological reserve of the numerical model is calculated to be 173 × 10^4 t. The actual geological reserves are 181 × 10^4 t. The error between the reserves calculated by the numerical model and the actual reserves is 4.42%. Therefore, the established numerical model is accurate.

2.4. Design of huff-n-puff schemes

The parameters used to establish the numerical model were all

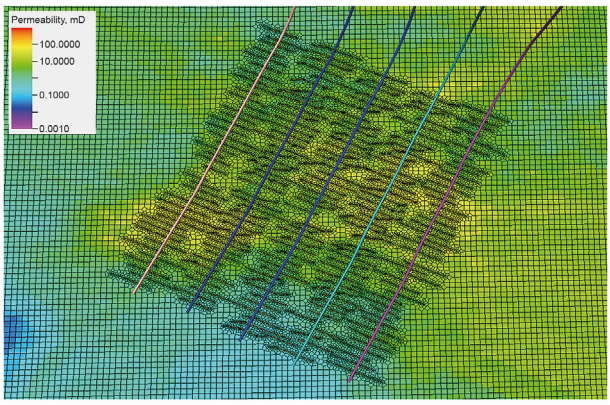

(a) Permeability

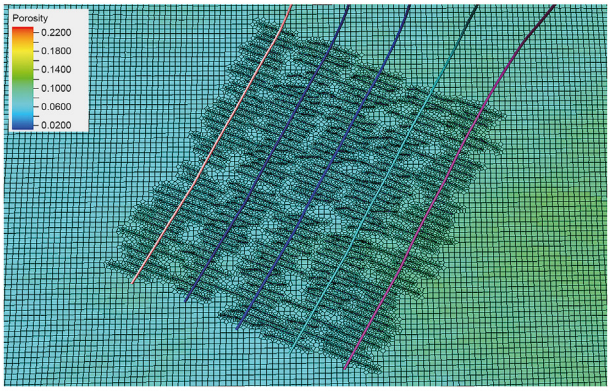

(b) Porosity

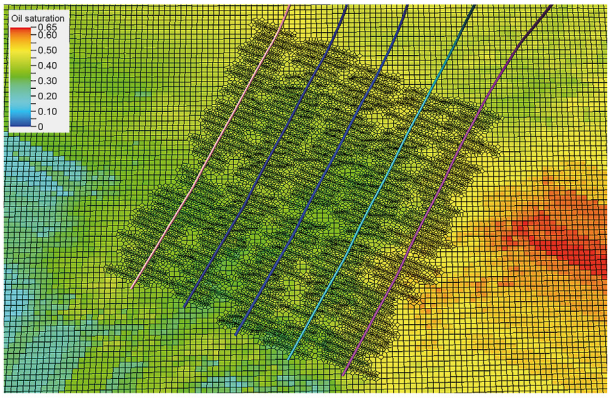

(c) Oil saturation

Fig. 7. Reservoir permeability, porosity, and oil saturation in the numerical model.

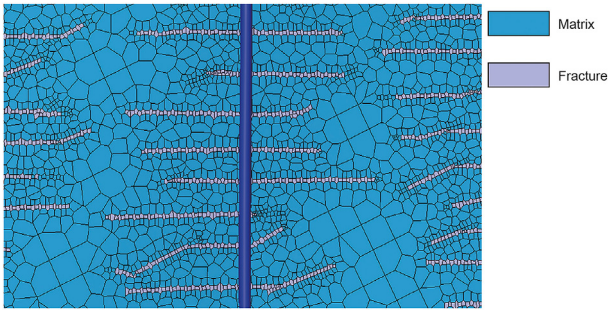

Fig. 8. The partitioning of fracture and matrix.

derived from oilfield data. The reservoir pressure and temperature are 35 MPa and 97.8 °C, respectively, with a saturation pressure of 3.87 MPa.

The EOR performance can be evaluated based on a change of incremental cumulative oil production and oil-exchanged rate in 5 years of hydrocarbon gas huff-n-puff. The oil-exchanged rate (R) is defined as the ratio of the cumulative increased oil production to the cumulative gas injection. The calculation equation of the oil-exchanged rate is shown in Eq. (2).

$$R = \frac{C_i}{C_g} \tag{2}$$

where C_i is the cumulative increased oil production, 10^4 t; C_g is cumulative gas injection, 10^4 t; R is oil-exchanged rate, t/t.

The study uses single-factor analysis to analyze the effect of individual parameter compared with primary depletion. The ranges of each parameter can be designed base on the known production parameters. Table 6 displays specific parameters of gas huff-n-puff.

The oil and water relative permeability curves of matrix and fracture are shown in Fig. 9, and the gas and oil relative permeability curves of matrix and fracture are shown in Fig. 10.

3. Optimization of injection–production parameters

After establishing the numerical model of hydrocarbon gas huff-n-puff considering complex fracture networks, the parameter of hydrocarbon gas huff-n-puff is optimized, which can provide engineers guidance for the development of unconventional oil reservoirs. The significant factors include gas injection time, single-well cumulative gas injection, injection rates, daily oil production, soaking time, and huff-n-puff cycles.

3.1. Gas injection time

The gas injection time was determined according to the initial reservoir pressure. Four comparison schemes were set up (80%, 70%, 60% and 55% of the original formation pressure) to analyze oil production performance. The single-well cumulative gas injection is 1000 t, and the oil production rate is 45 m^3/d.

The change rule of gas injection time and cumulative oil production is shown in Fig. 11. Although higher oil production can be obtained by later gas injection, the cumulative oil production is increased by 0.05% when it occurs after the formation pressure has fallen from 60% to 55% relative to the original formation pressure.

The period of stable oil production becomes longer, and the daily oil production declines slower by earlier gas injection as shown in Fig. 12. When gas injection is started at 60% of the initial formation pressure, the period of stable oil production is less than three months. Therefore, gas injection is started at 60% of the original formation pressure for target unconventional reservoirs, which is beneficial for EOR by hydrocarbon gas huff-n-puff.

Fig. 13 illustrates that the formation pressure drops significantly after soaking by later gas injection. Gas injection interferes with oil production during high formation pressure. Gas injection into the formation can effectively replenish energy and improve oil recovery. The formation pressure increases as the hydrocarbon gas continues to be injected. And high formation pressure reduces the effective sweeping volume of the injected gas and makes it difficult to dissolve the crude oil far away from the wellbore. Therefore, high formation pressure is not beneficial for EOR.

3.2. Cumulative gas injection (single well)

The most significant cumulative gas injection (single-well) are

Table 6
Parameters of the huff-n-puff.

Parameter	Value	Basic case
Gas injection time, %	80, 70, 60, 55	60
Cumulative gas injection (single-well), t	500, 1000, 1500, 2000, 2500, 3000	1000
Gas injection rate, t/d	20, 50, 100, 200, 250	100
Soaking time, d	5, 10, 15, 30, 45, 60	10
Daily oil production rate, t/d	10, 15, 20, 25, 30, 45	45
Huff-n-puff cycle	1, 2, 3, 4, 5, 6	1

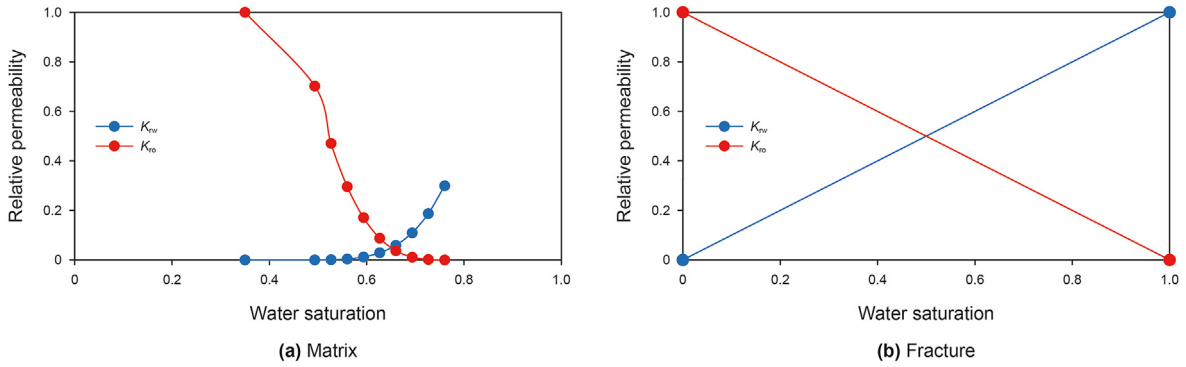

Fig. 9. Oil and water relative permeability curves.

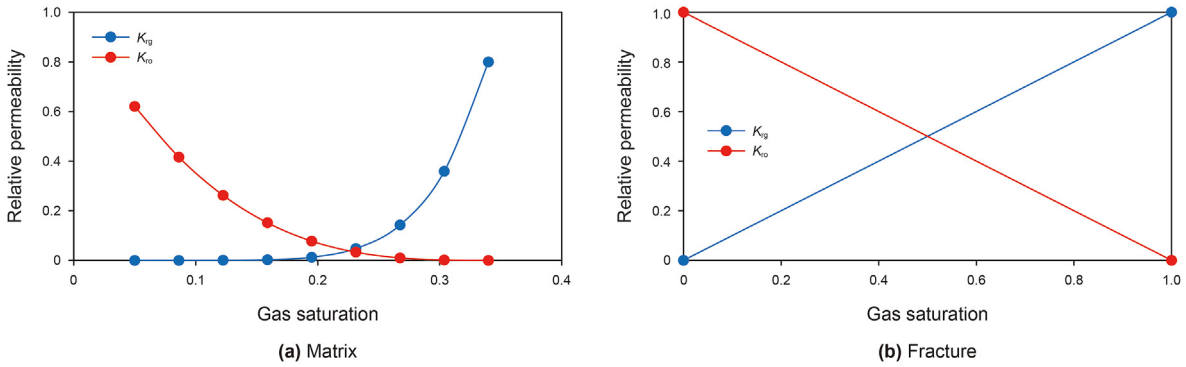

Fig. 10. Gas and oil relative permeability curves.

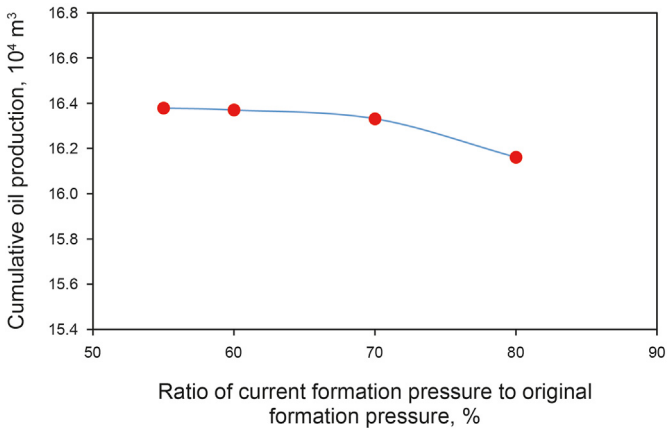

Fig. 11. Cumulative oil production under different gas injection time.

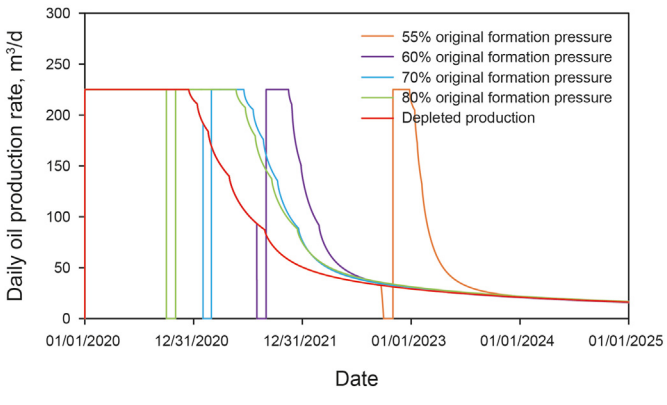

Fig. 12. Daily oil production rates under different gas injection time.

obtained by altering the single-well cumulative gas injection (200, 500, 1000, 1500, 2000, 2500, 3000 t). Each scheme starts with gas injection at 60% of the initial formation pressure, and other conditions remain unchanged.

Fig. 14 shows that as the increase in single-well cumulative gas

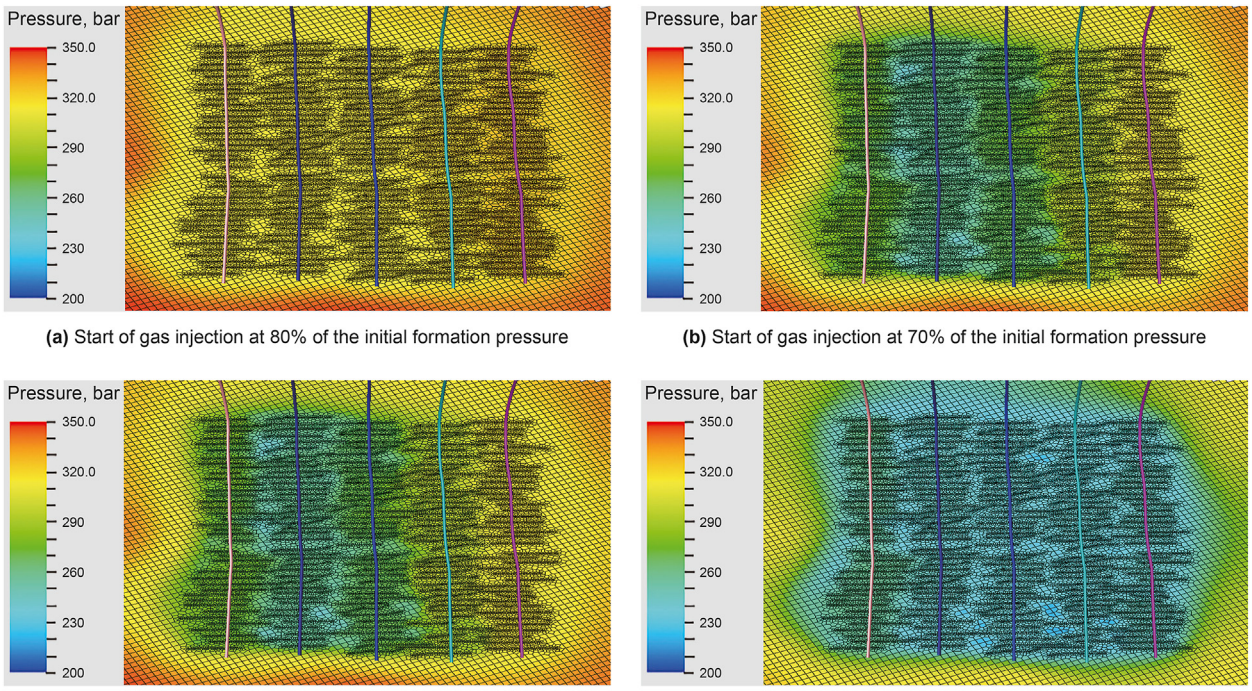

Fig. 13. Formation pressure distribution at the end of the soaking.

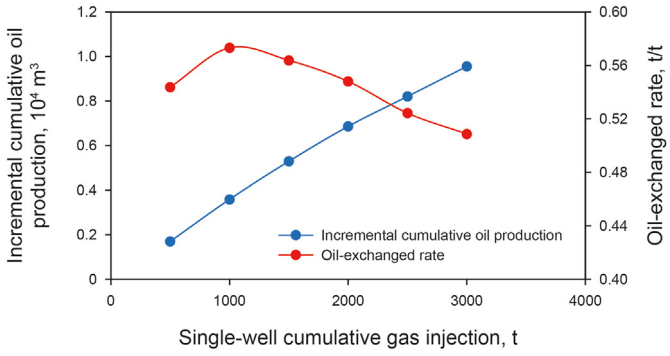

Fig. 14. Incremental cumulative oil production and oil-exchanged rates under different cumulative gas injection (single well).

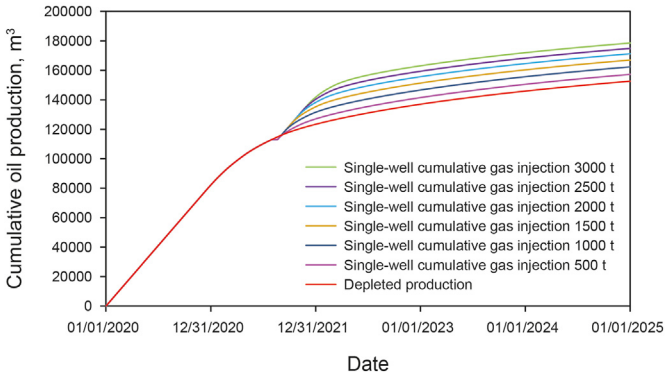

Fig. 15. Cumulative oil production under different cumulative gas injection (single-well).

injection (from 500 to 3000 t), the incremental cumulative oil-production rate is gradually increased by 7.86 × 10^4 m^3. In the same changes, the oil-exchanged rate first rises and then falls, wherein the oil-exchanged rate approaches its highest point when the single-well cumulative gas injection reaches 1000 t.

Figs. 15 and 16 show that the EOR performance significantly improves as the gas injection rate (single well) increases. The period of steady oil production after soaking becomes longer with higher single-well cumulative gas injection rates (Fig. 15). The oil production rate declines rapidly when the cumulative gas injection for a single well is less than 500 t. High bottom hole pressure can lead to a rapid drop in pressure during soaking. Therefore, the single-well cumulative gas injection of 1000 t can yield good oil production performance.

As the cumulative hydrocarbon gas injection accumulates, the range of hydrocarbon gas sweep becomes wider, and the oil saturation around the bottom hole decreases rapidly (Fig. 17). Under high bottom hole pressure, crude oil with dissolved hydrocarbon

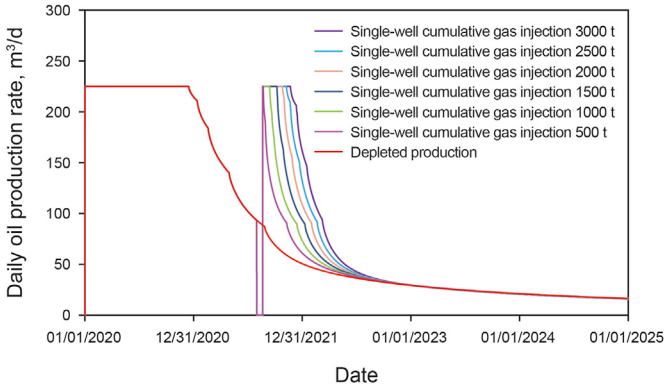

Fig. 16. Daily oil production rates under different cumulative gas injection (single well).

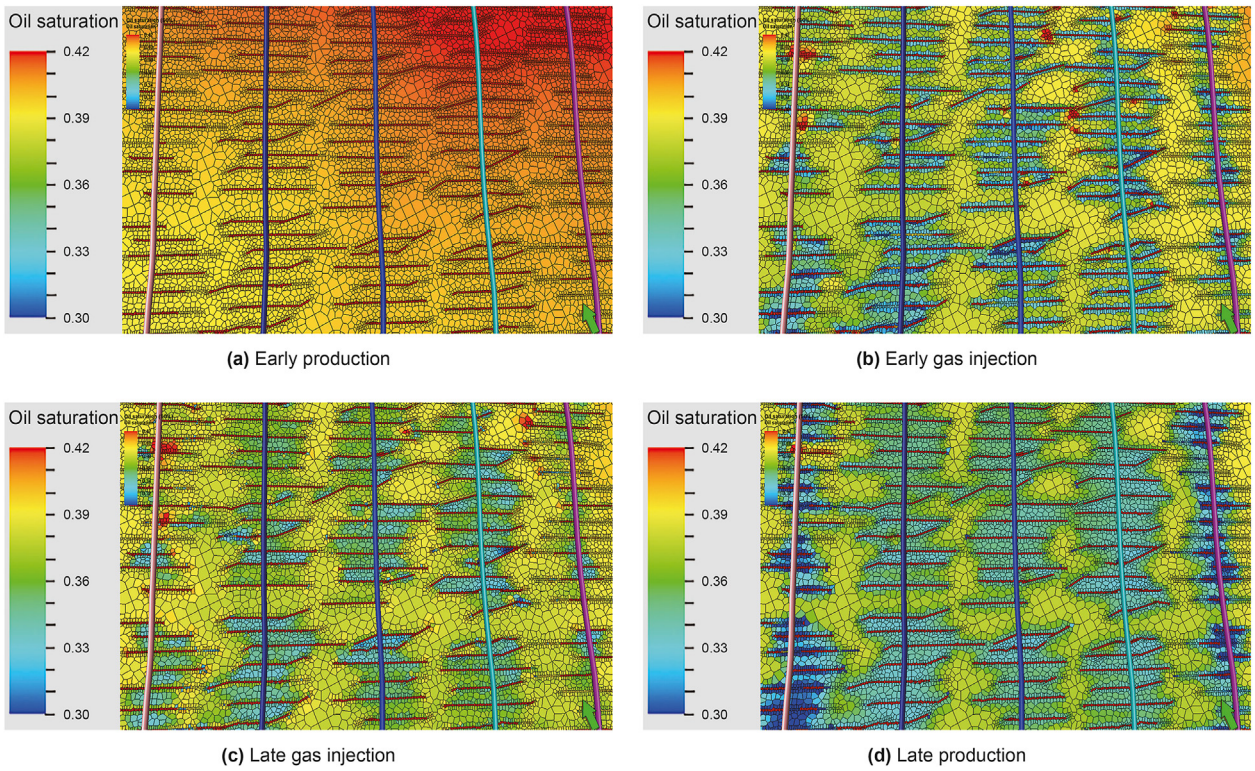

Fig. 17. Variation in oil saturation of hydrocarbon gas huff-n-puff of cumulative gas injection of 1000 t (single-well).

gas near the end of the well is pushed away from the producing well, which can cause a rapid decrease in oil saturation. High bottom hole pressure is not beneficial to EOR.

3.3. Gas injection rate

The hydrocarbon gas injection rates required for analysis after the optimal injection time (started at 60% of the initial formation pressure) and single-well cumulative gas injection (1000 t) are determined. Five sets of gas injection rates are devised, that is 20, 50, 100, 200, 250 t/d, and other conditions remain unchanged.

Fig. 18 shows the increase in oil-exchanged rate and incremental cumulative oil production as the hydrocarbon gas injection rate increases from 20 to 50 t/d, while they decline when the hydrocarbon gas injection rate exceeds 100 t/d. The oil-exchanged rate reaches 0.573 t/t when the gas injection rates are 50 and 100 t/d.

Through observation, compared to cumulative gas injection

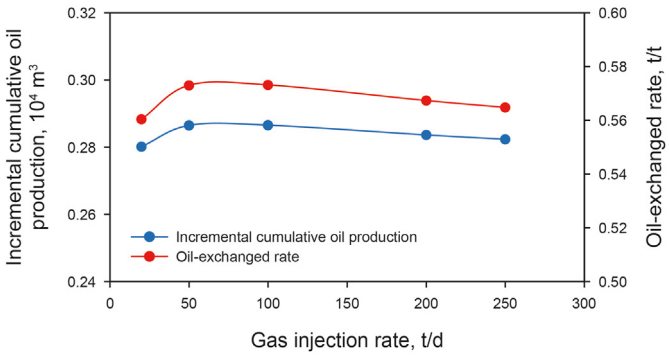

Fig. 18. Incremental cumulative oil production and oil-exchanged rates under different gas injection rates.

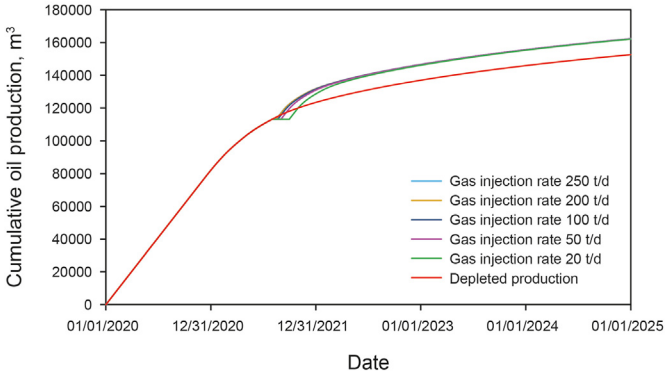

Fig. 19. Cumulative oil production under different gas injection rates.

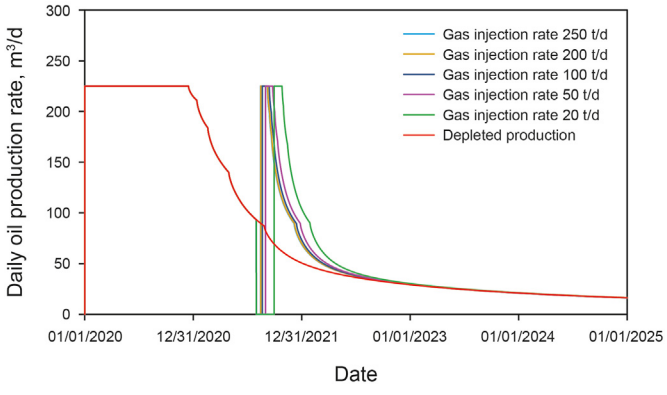

Fig. 20. Daily oil production rates under different gas injection rates.

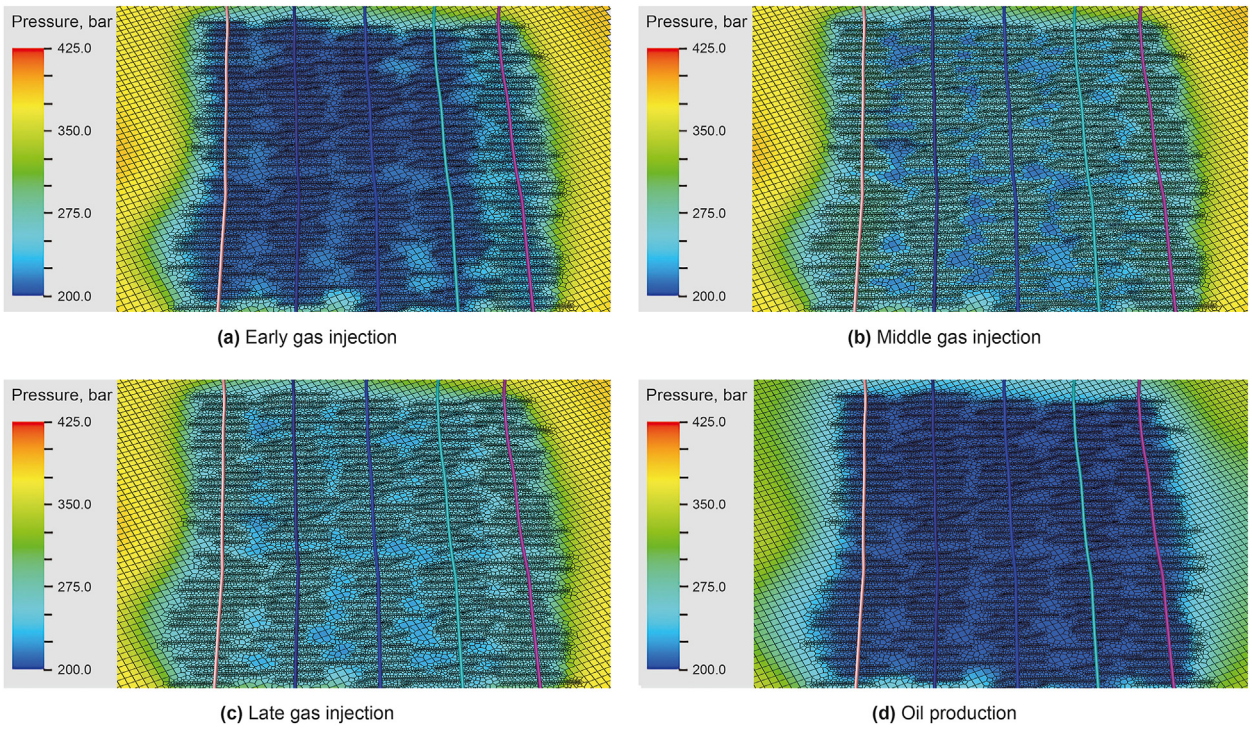

Fig. 21. Reservoir pressure variation of gas huff-n-puff at gas injection rate of 100 t/d.

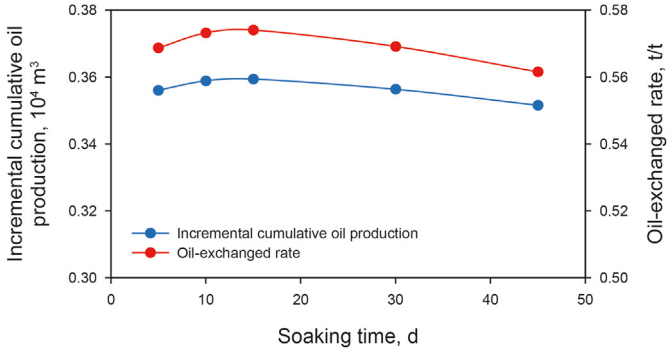

Fig. 22. Incremental cumulative oil production and oil-exchanged rates under different soaking time.

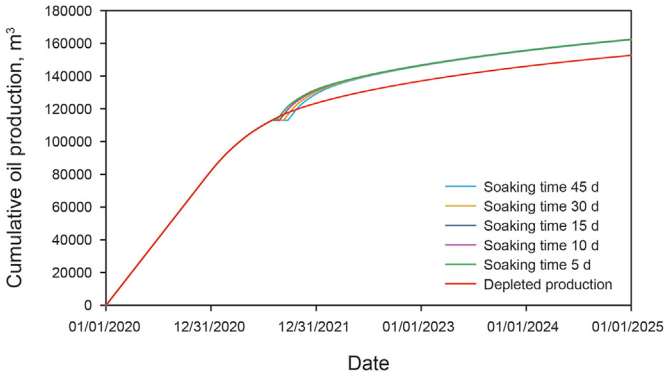

Fig. 23. Cumulative oil production under different soaking time.

rates (single-well), the impact of gas injection rate on oil recovery is minimal (Figs. 19 and 20). When the injection rate reaches 250 t/d, the bottom hole pressure approaches 34 MPa, which makes it easy to quickly push crude oil containing a large amount of dissolved hydrocarbon gas out of the near-wellbore zone. In order to improve oil recovery, the optimal gas injection rate is 50–100 t/d.

The bottom hole pressure rises rapidly as the gas injection rate increases, and the formation fluid achieves a miscible phase, shown in Fig. 21. The high injection rate inhibits hydrocarbon gas diffusion, and the bottom hole pressure rises rapidly. Due to high injection rates, surface equipment requirements have become more stringent, increasing the economic cost of reservoir development.

3.4. Soaking time

Five types of soaking time (5, 10, 15, 30, and 45 d) are designed to investigate the impact of soaking time on production performance. After depletion, gas injection begins at 60% of the initial formation

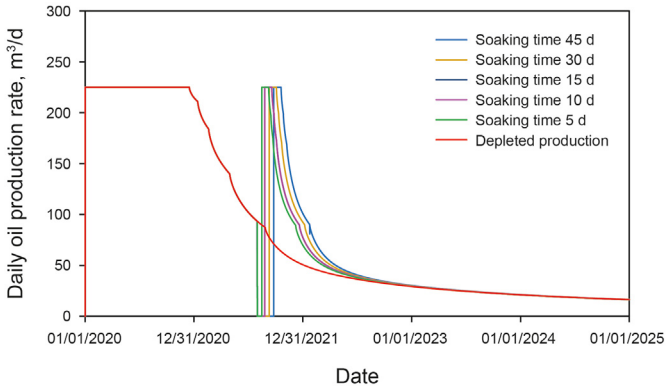

Fig. 24. Daily oil production rates under different soaking time.

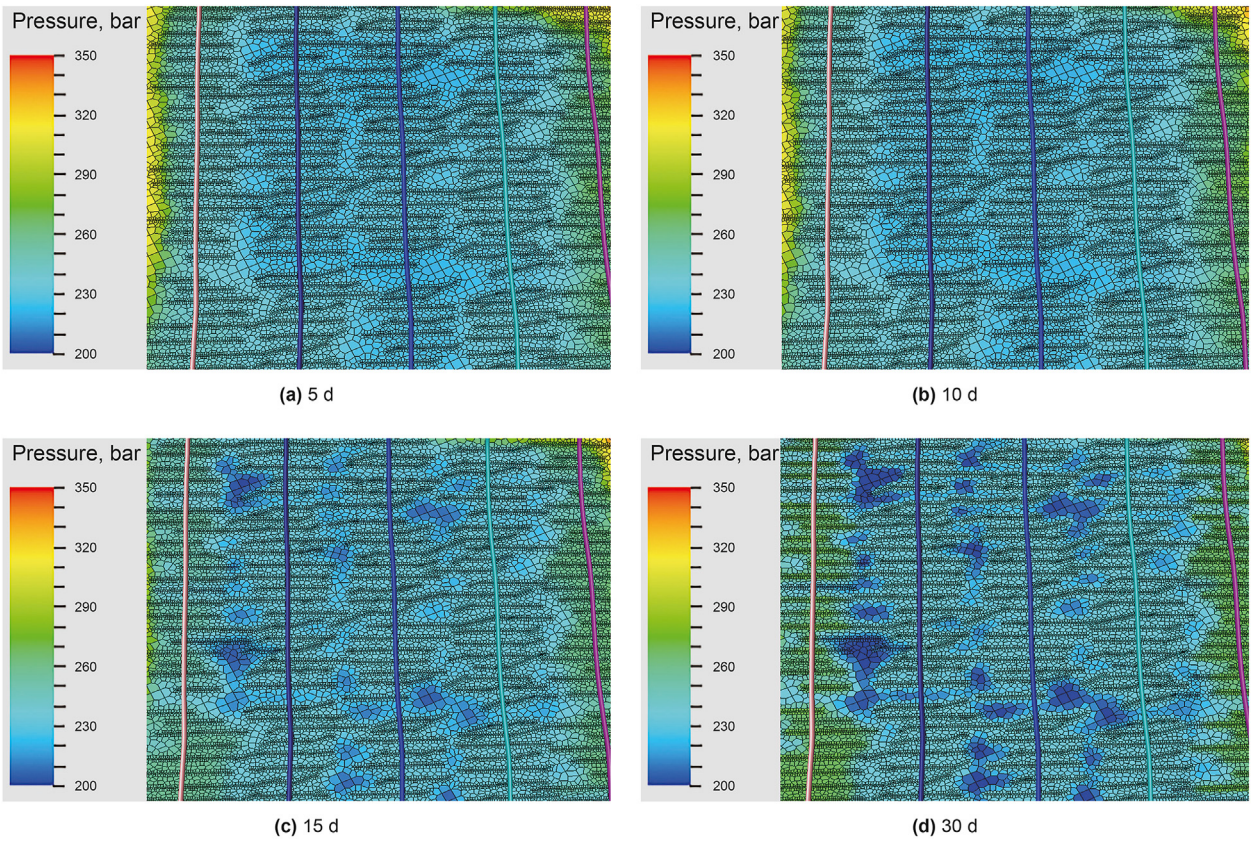

Fig. 25. Reservoir pressure at the end of soaking at different soaking time.

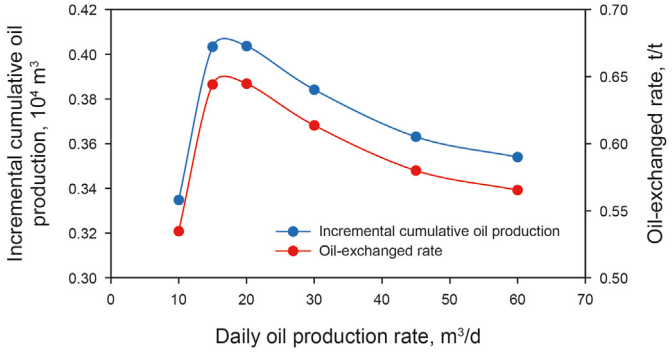

Fig. 26. Incremental cumulative oil production and oil-exchanged rates under different daily oil production rates.

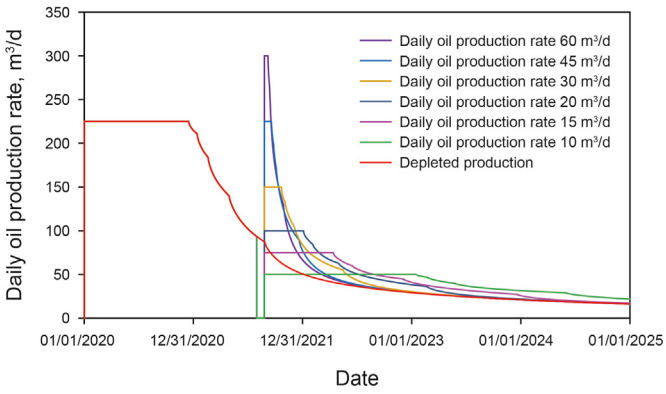

Fig. 28. Different daily oil production rates.

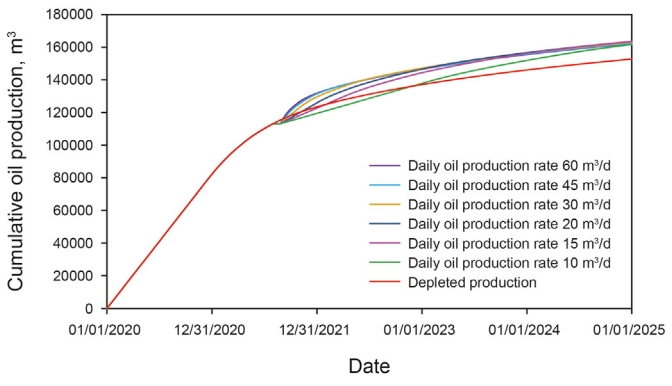

Fig. 27. Cumulative oil production under different daily oil production rates.

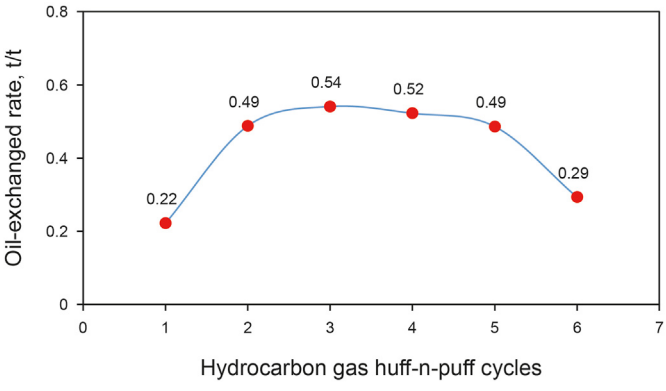

Fig. 29. Oil-exchanged rates under different hydrocarbon gas huff-n-puff cycles.

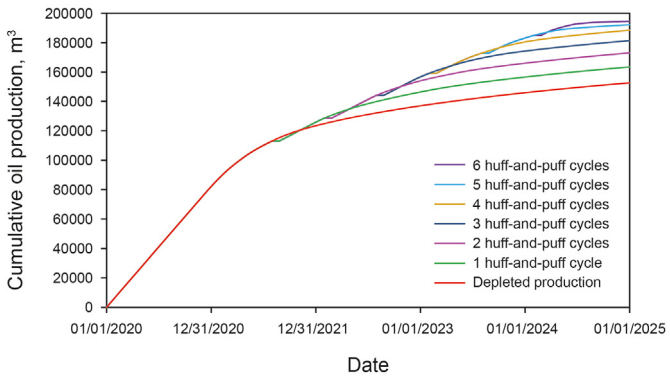

Fig. 30. Cumulative oil production under different hydrocarbon gas huff-n-puff cycles.

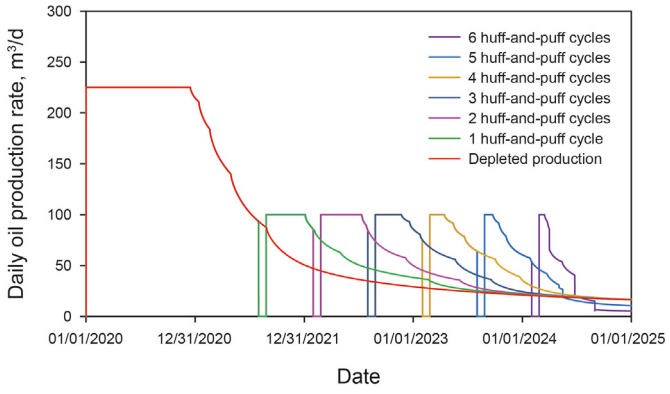

Fig. 31. Daily oil production rates under different hydrocarbon gas huff-n-puff cycles.

pressure. The single-well cumulative gas injection is set as 1000 t, with other conditions remaining unchanged.

Fig. 22 indicates that a soaking time of 15 d will result in the highest oil-exchanged rate and incremental cumulative oil production. The incremental cumulative oil production is increased by 70 t, and the oil-exchanged rate is enhanced by 0.015 t/t when the soaking time is altered from 5 to 15 d. The influence of gas huff-n-puff can be inferred that soaking time has minimal effect on hydrocarbon gas huff-n-puff.

As the soaking time increases, the cumulative oil production for different soaking times is almost the same (Fig. 23). The period of steady oil production become longer, and the production decline rate becomes slower by longer soaking time as illustrated in Fig. 24. The oil-exchange rate rises to 0.574 t/t after 15 d of soaking.

The formation pressure decreases significantly with the prolongation of soaking time (Fig. 25). Hydrocarbon gas and crude oil are completely dissolved, and as the soaking time prolongs, the production performance of gas injection in increasing reservoir pressure is poor. Short soaking time can lead to the insufficient dissolution of injected gas and oil, resulting in poor oil production efficiency.

3.5. Daily oil production rate

Six daily oil production rates (10, 15, 20, 30, 45, and 60 m^3/d) are designed to analyze the oil production performance of the hydrocarbon gas huff-n-puff. Other conditions remain unchanged.

When the oil production is maintained at 20 m^3/d, the highest oil-exchanged rate and incremental cumulative oil production rate can be attained. When the daily oil production rate climbs from 10 to 20 m^3/d, the incremental oil production is increased by 690 m^3, and the oil-exchanged rate is increased by 0.11 t/t (Fig. 26).

The growth in incremental cumulative oil production is less than 1.4% with the increase in daily oil production (Fig. 27). At the same time, the period of steady oil production becomes shorter. The rate of decreasing production becomes faster with higher daily oil production rate (Fig. 28). The highest oil production rate for M oil reservoir is approximately 15–20 m^3/d.

3.6. Gas huff-n-puff cycles

Six cases are designed, with gas huff-n-puff cycles ranging from 1 to 6. In each cycle, the single-well cumulative gas injection is maintained at 1000 t, and the single-well hydrocarbon gas injection rate is 100 t/d. It is started at 60% of the original formation pressure, and the oil production rate is 20 m^3/d. Other conditions remain unchanged.

When the gas huff-n-puff cycles change from 1 to 3, the oil-exchanged rate rises to 0.32 t/t. In contrast, when the huff-n-puff cycles change from 3 to 6, the oil-exchanged rate significantly drops (Fig. 29). The cumulative gas injection in a single cycle remained constant as huff-n-puff cycles continue to increase, but the incremental cumulative oil production decreases since the near-well zone gets less saturated with crude oil after several cycles of hydrocarbon gas huff-n-puff, resulting in less effective for EOR. In general, gas huff-n-puff for 3–4 cycles yield good EOR performance with an oil-exchange rate of 0.52–0.54 t/t per cycle.

Fig. 30 demonstrates that cumulative oil production increases with rising gas huff-n-puff cycles. The steady production of single-cycle oil production rates decline by more hydrocarbon gas huff-n-puff cycles can be seen in Fig. 31. The bottom hole pressure drops fast during each cycle, and the oil enhancement effect degrades after too many cycles of gas huff-n-puff. As a result, the ideal cycle for hydrocarbon gas huff-n-puff is 3–4 cycles.

The oil saturation after each gas huff-n-puff cycle is shown in Fig. 32. The oil saturation around fractures near the wellbore drops with more frequent gas huff-n-puff cycles. The viscosity of formation oil gradually drops as it approaches the well bottom, and the range of the viscosity reduction grows as the region of hydrocarbon gas wave area increases. Increasing the huff-n-puff cycle can significantly improve incremental cumulative oil production. For the M unconventional reservoir, maximal oil improvement can be achieved by 3–4 cycles of hydrocarbon gas huff-n-puff.

4. Dominated factor analysis

4.1. Range analysis

This work analyzes the dominant factors of injection–production parameters by utilizing a range analysis approach with increased oil as the evaluation indicator. The extreme difference in incremental cumulative oil production was obtained by subtracting the highest and minimum values of incremental cumulative oil production for each parameter to assess the sensitivity of the injection–production parameters. The conclusion is that the most sensitive factor of oil enhancement through hydrocarbon gas huff-n-puff is gas injection time, followed by single-well cumulative gas injection and daily oil production (Fig. 33).

4.2. Hierarchical analysis

Based on the analytic hierarchy process (AHP), the incremental cumulative oil production changes derived from the extreme difference analysis method are used as evaluation criteria for different

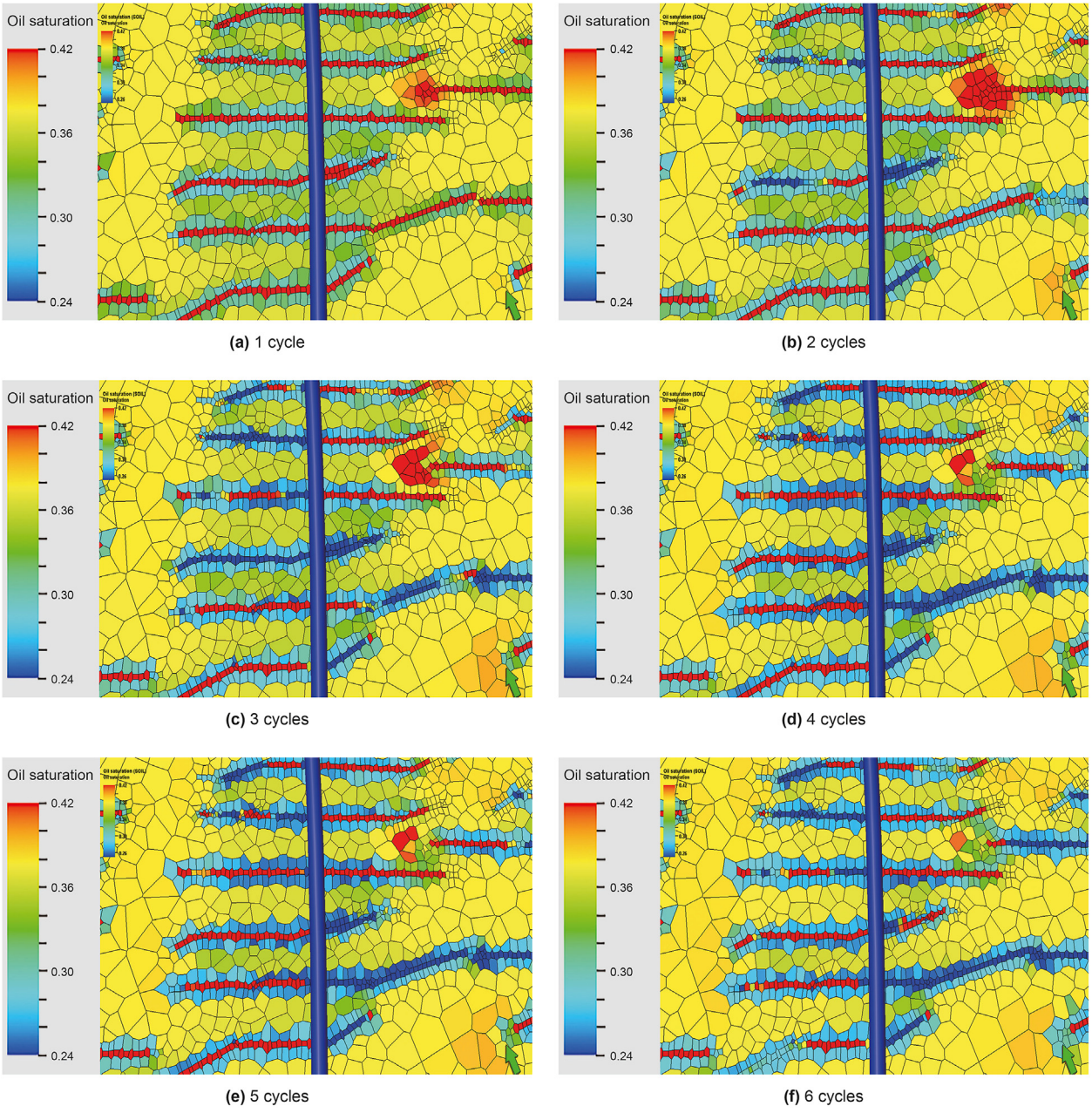

Fig. 32. Oil saturation at the end of individual gas huff-n-puff cycles.

injection–production parameters, and a discriminant matrix of injection-production parameters is constructed. Fig. 34 shows the flowchart of the hierarchical analysis.

Table 7 lists the relative weight values $\boldsymbol{A} = [0.40, 0.28, 0.07, 0.05, 0.20]^{T}$ of the injection–production parameters on incremental cumulative oil production. The consistency test analysis yielded CR = 0.025 < 0.1, which proved that the injection–production parameter matrix passed the test, and the weight values met the requirements.

Gas injection time is the critical sensitive factor among the injection–production parameter with a weight of 0.40, followed by single-well cumulative gas injection (with a weight of 0.28).

5. Conclusions

This work develops a numerical model of hydrocarbon gas huff-n-puff of multiple MFHWs with complex fracture networks to obtain the optimal injection–production parameters. The fuzzy hierarchical analysis is used to determine the dominant factors of hydrocarbon gas huff-n-puff, which provides theoretical guidance for the hydrocarbon gas huff-n-puff in MFHW under complex fracture networks.

(1) In the M oil reservoir, the MMP for hydrocarbon gas is 33.5 MPa from the simulation of slim tube, and the current pressure of hydrocarbon gas injection can achieve miscible displacement. The cumulative oil production of hydrocarbon gas huff-n-puff is 17.4×10^4 m^3. The incremental cumulative

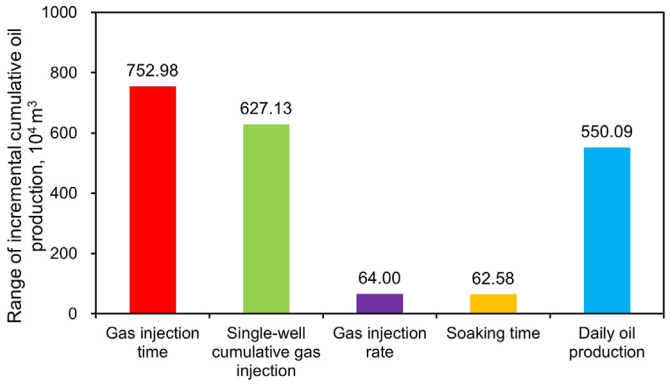

Fig. 33. Range of incremental cumulative oil production with different injection–production parameters.

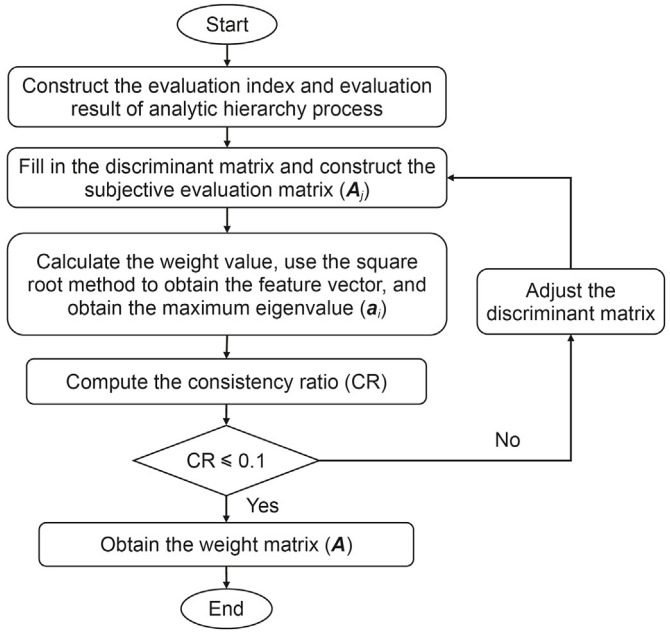

Fig. 34. Flowchart of the hierarchical analysis.

Table 7
Discriminant matrix of incremental cumulative oil production by injection–production parameters.

	Gas injection time	Single-well cumulative gas injection	Gas injection rate	Soaking time	Daily oil production rate	Weight
Gas injection time	1	2	6	6	2	0.40
Single-well cumulative gas injection	1/2	1	5	5	2	0.28
Gas injection rate	1/6	1/5	1	2	1/4	0.07
Soaking time	1/6	1/5	1/2	1	1/4	0.05
Daily oil production rate	1/2	1/2	4	4	1	0.20

oil production is 1.05×10^4 m^3 compared with primary depletion.

(2) Hydrocarbon gas huff-n-puff beginning at 60% of the original formation pressure after depletion is beneficial for EOR. The optimal injection and production parameters include the cumulative gas injection of an individual well (1000 t), gas injection rate (50–100 t/d), soaking time per cycle (10–15 d), and daily oil production rate after gas injection (15–20 m^3/d). Overall, 3 to 4 cycles can yield good EOR performance.

(3) Incremental cumulative oil production is used the evaluation indicator of injection–production parameters. In addition, the key factor of hydrocarbon gas huff-n-puff considering complex fracture networks is gas injection time (with a weight of 0.40), followed by cumulative gas injection of single-well (with a weight of 0.28).

CRediT authorship contribution statement

Hao-Chuan Zhang: Formal analysis, Methodology, Writing – original draft. **Yong Tang:** Conceptualization, Funding acquisition, Supervision. **You-Wei He:** Methodology, Supervision, Writing – review & editing. **Yong Qin:** Data curation, Resources, Validation. **Jian-Hong Luo:** Writing – review & editing. **Yu Sun:** Visualization. **Ning Wang:** Writing – original draft. **De-Qiang Wang:** Formal analysis.

Declaration of competing interest

The authors declare that they have no known competing financial interests or personal relationships that could have appeared to influence the work reported in this paper.

Acknowledgements

This work was funded by the National Natural Science Foundation of China (No. 51974268), Open Fund of Key Laboratory of Ministry of Education for Improving Oil and Gas Recovery (NEPU-EOR-2022-03) and Research and Innovation Fund for Graduate Students of Southwest Petroleum University (No. 2022KYCX005).

References

Bealessio, B.A., Alonso, N.A.B., Mendes, N.J., et al., 2021. A review of enhanced oil recovery (EOR) methods applied in Kazakhstan. Petroleum 7 (1), 1–9. https://doi.org/10.1016/j.petlm.2020.03.003.

Chen, H., Yao, C., Datta-Gupta, A., et al., 2020. Identification of fractures and preferential flow paths using streamlines and dynamic data in dual porosity dual permeability reservoir models. In: SPE Annual Technical Conference and Exhibition. https://doi.org/10.2118/201277-MS.

Cheng, S., Wang, Y., Lang, H., et al., 2017. Feasibility of inter-fracture injection and production for the same multistage fractured horizontal well in tight oil reservoir. Acta Pet. Sin. 38 (12), 1411. https://doi.org/10.7623/syxb201712008 (in Chinese).

Cockin, A.P., Malcolm, L.T., McGuire, P.L., et al., 2000. Analysis of a single-well chemical tracer test to measure the residual oil saturation to a hydrocarbon miscible gas flood at Prudhoe Bay. SPE Reservoir Eval. Eng. 3 (6), 544–551. https://doi.org/10.2118/68051-PA.

Ding, M., Gao, M., Wang, Y., et al., 2019. Experimental study on CO_2-EOR in fractured reservoirs: influence of fracture density, miscibility and production scheme. J. Petrol. Sci. Eng. 174, 476–485. https://doi.org/10.1016/j.petrol.2018.11.039.

Ding, M., Li, Q., Yuan, Y., et al., 2022. Permeability and heterogeneity adaptability of surfactant-alternating-gas foam for recovering oil from low-permeability reservoirs. Petrol. Sci. 19 (3), 1185–1197. https://doi.org/10.1016/j.petsci.2021.12.018.

Feng, Q., Jiang, Z., Wang, S., et al., 2019. Optimization of reasonable production pressure drop of multi-stage fractured horizontal wells in tight oil reservoirs. J. Pet. Explor. Prod. Technol. 9 (3), 1943–1951. https://doi.org/10.1007/s13202-018-0586-5.

Fu, J., Chen, H., Yao, C., et al., 2023. Field application of a novel multi-resolution multi-well unconventional reservoir simulation: history matching and

parameter identification. In: SPE/AAPG/SEG Unconventional Resources Technology Conference. https://doi.org/10.15530/urtec-2023-3857125.
Fu, Q., Cudjoe, S., Ghahfarokhi, R.B., et al., 2021. Investigating the role of diffusion in hydrocarbon gas huff and puff injection– an Eagle Ford study. J. Petrol. Sci. Eng. 198, 108146. https://doi.org/10.1016/j.petrol.2020.108146.
Haines, H.K., Monger, T.G., 1990. A laboratory study of natural gas huff 'n' puff. In: CIM/SPE International Technical Meeting. https://doi.org/10.2118/21576-MS.
Hao, M., Liao, S., Yu, G., et al., 2020. Performance optimization of CO_2 huff-n-puff for multifractured horizontal wells in tight oil reservoirs. Geofluids. https://doi.org/10.1155/2020/8840384.
He, Y., Qin, J., Cheng, S., Chen, J., 2020. Estimation of fracture production and water breakthrough locations of multi-stage fractured horizontal wells combining pressure-transient analysis and electrical resistance tomography. J. Petrol. Sci. Eng. 194, 107479. https://doi.org/10.1016/j.petrol.2020.107479.
He, Y., Qiao, Y., Qin, J., et al., 2022. A novel method to enhance oil recovery by inter-fracture injection and production through the same multi-fractured horizontal well. J. Energy Resour. Technol. 144 (4). https://doi.org/10.1115/1.4051623.
He, Y., He, Z., Tang, Y., Xu, Y., Long, J., Sepehrnoori, K., 2023a. Shale gas production evaluation framework based on data-driven models. Petrol. Sci. 20 (3), 1659–1675. https://doi.org/10.1016/j.petsci.2022.12.003.
He, Y., He, Z., Tang, Y., et al., 2023b. Interwell fracturing interference evaluation in shale gas reservoirs. Geoenergy Science and Engineering, 212337. https://doi.org/10.1016/j.geoen.2023.212337.
Hu, W., Wei, Y., Bao, J., 2018. Development of the theory and technology for low permeability reservoirs in China. Petrol. Explor. Dev. 45 (4), 685–697. https://doi.org/10.1016/S1876-3804(18)30072-7.
Jing, W., Liu, H., Qian, G., et al., 2021. Mechanisms and capacity of high-pressure soaking after hydraulic fracturing in tight/shale oil reservoirs. Petrol. Sci. 18, 546–564. https://doi.org/10.1007/s12182-020-00524-z.
Lei, Z., Li, J., Chen, Z., et al., 2023. Characterization of multiphase flow in shale oil reservoirs considering multiscale porous media by high-resolution numerical simulation. SPE J. 1–16. https://doi.org/10.2118/215847-PA.
Li, Y., Shi, J., Nie, M., et al., 2023. Drill string dynamic characteristics simulation for the ultra-deep well drilling on the south margins of Junggar Basin. Petroleum 9 (2), 205–213. https://doi.org/10.1016/j.petlm.2021.10.011.
Lino, U.D.R., 1994. An evaluation of natural gas huff and puff field tests in Brazil. In: SPE Latin America and Caribbean Petroleum Engineering Conference. https://doi.org/10.2118/26974-MS.
Ming, C., Zhang, S., Yun, X., et al., 2020. A numerical method for simulating planar 3D multi-fracture propagation in multi-stage fracturing of horizontal wells. Petrol. Explor. Dev. 47 (1), 171–183. https://doi.org/10.1016/S1876-3804(20)60016-7.
Mohammed–Singh, L., Singhal, A.K., Sim, S., 2006. Screening criteria for CO_2 huff 'n' puff operations. In: SPE/DOE Symposium on Improved Oil Recovery. https://doi.org/10.2118/100044-MS.
Ozowe, W., Zheng, S., Sharma, M., 2020. Selection of hydrocarbon gas for huff and puff IOR in shale oil reservoirs. J. Petrol. Sci. Eng. 195, 107683. https://doi.org/10.1016/j.petrol.2020.107683.
Pu, W., Bing, W., Jin, F., et al., 2016. Experimental investigation of CO_2 huff and puff process for enhancing oil recovery in tight reservoirs. Chem. Eng. Res. Des. 111, 269–276. https://doi.org/10.1016/j.cherd.2016.05.012.
Qin, J., Zhong, Q., Tang, Y., Yu, W., Sepehrnoori, K., 2023. Well interference evaluation considering complex fracture networks through pressure and rate transient analysis in unconventional reservoirs. Petrol. Sci. 20 (1), 337–349. https://doi.org/10.1016/j.petsci.2022.09.029.
Sie, C., Nguyen, Q.P., 2022. Laboratory experiments of field gas huff and puff for improving oil recovery from Eagle Ford Shale reservoirs. Arabian J. Geosci. 15 (21), 1–13. https://doi.org/10.2118/200471-MS.
Sumeer, K., Wei, T., Wu, X., 2018. A numerical simulation study of CO_2 injection for enhancing hydrocarbon recovery and sequestration in liquid-rich shales. Petrol. Sci. 15, 103–115. https://doi.org/10.1007/s12182-017-0199-5.
Sun, K., Liu, H., Wang, J., et al., 2022. Three-dimensional physical simulation of water huff and puff in a tight oil reservoir with stimulated reservoir volume. J. Petrol. Sci. Eng. 208, 109212. https://doi.org/10.1016/j.petrol.2021.109212.
Tang, Y., Hou, C., He, Y., et al., 2021a. Review on pore structure characterization and microscopic flow mechanism of CO_2 flooding in porous media. Energy Technol. 9 (1), 2000787. https://doi.org/10.1002/ente.202000787.
Tang, Y., Chen, Y., He, Y., et al., 2021b. An improved system for evaluating the adaptability of natural gas flooding in enhancing oil recovery considering the miscible ability. Energy 236. https://doi.org/10.1016/j.energy.2021.121441.
Tang, Y., Zhang, H., He, Y., et al., 2022. A novel type curve for estimating oil recovery factor of gas flooding. Petrol. Explor. Dev. 49 (3), 605–613. https://doi.org/10.1016/S1876-3804(22)60050-8.
Torabi, F., Asghari, K., 2010. Effect of operating pressure, matrix permeability and connate water saturation on performance of CO_2 huff-and-puff process in matrix-fracture experimental model. Fuel 89 (10), 2985–2990. https://doi.org/10.1016/j.fuel.2010.05.020.
Wang, J., Zhang, S., 2018. Pore structure differences of the extra-low permeability sandstone reservoirs and the causes of low resistivity oil layers: a case study of Block Yanwumao in the middle of Ordos Basin, NW China. Petrol. Explor. Dev. 45 (2), 273–280. https://doi.org/10.1016/S1876-3804(18)30030-2.
Wang, S., Li, X., Hao, L., et al., 2022. Proactive stress interference mechanism and its application in the Mahu oil area, Junggar basin. Front. Earth Sci. 10, 948932. https://doi.org/10.3389/feart.2022.948932.
Wang, Z., Sun, B., Guo, P., et al., 2021. Investigation of flue gas water-alternating-gas (flue gas-WAG) injection for enhanced oil recovery and multicomponent flue gas storage in the post-waterflooding reservoir. Petrol. Sci. 18, 870–882. https://doi.org/10.1007/s12182-021-00548-z.
Xiong, Q., Ma, X., Wu, B., et al., 2022. Re-fracturing wells selection by fuzzy comprehensive evaluation based on analytic hierarchy process– Taking Mahu Oilfield as an example. Front. Energy Res. 10, 851582. https://doi.org/10.3389/fenrg.2022.851582.
Yan, Z., Li, X., Zhu, X., et al., 2023. MD-CFD simulation on the miscible displacement process of hydrocarbon gas flooding under deep reservoir conditions. Energy 263, 125730. https://doi.org/10.1016/j.energy.2022.125730.
Zhang, Y., Yang, D., 2021. Modeling transient pressure behaviour of a multi-fractured horizontal well in a reservoir with an arbitrary boundary and different fracture networks by considering stress-sensitive effect. J. Hydrol. 600, 126552. https://doi.org/10.1016/j.jhydrol.2021.126552.
Zhang, Y., Zou, Y., Zhang, Y., et al., 2022. Experimental study on characteristics and mechanisms of matrix pressure transmission near the fracture surface during post-fracturing shut-in in tight oil reservoirs. J. Petrol. Sci. Eng. 219, 111133. https://doi.org/10.1016/j.petrol.2022.111133.
Zhao, F., Fu, Z., Hao, H., et al., 2018. Mechanism of nitrogen foam preventing edge-water coning in huff and puff well. Oilfield Chem. 35 (3), 451–457. https://doi.org/10.19346/j.cnki.1000-4092.2018.03.014 (in Chinese).
Zhao, X., Liu, L., Hu, J., et al., 2014. The tectonic fracture modeling of an ultra-low permeability sandstone reservoir based on an outcrop analogy: a case study in the Wangyao Oilfield of Ordos Basin, China. Petrol. Sci. 11 (3), 363–375. https://doi.org/10.1007/s12182-014-0350-5.
Zhao, X., Rui, Z., Liao, X., 2016. Case studies on the CO_2 storage and EOR in heterogeneous, highly water-saturated, and extra-low permeability Chinese reservoirs. J. Nat. Gas Sci. Eng. 29, 275–283. https://doi.org/10.1016/j.jngse.2015.12.044.
Zheng, T., Liu, X., Yang, Z., et al., 2021. Identification of seepage mechanisms for natural gas Huff and puff and flooding processes in hydrophilic reservoirs with low and ultra-low permeabilities. J. Energy Resour. Technol. 143 (6), 063004. https://doi.org/10.1115/1.4048526.
Zhou, R., Su, Y., Ma, B., et al., 2020. CO_2 huff and puff simulation in horizontal well with random fractal volume fracturing. Lithologic Reservoirs 32 (1), 161–168. https://doi.org/10.12108/yxyqc.20200118 (in Chinese).